Biosensors and Bioelectronics 165 (2020) 112420

Contents lists available at ScienceDirect

Biosensors and Bioelectronics

journal homepage: http://www.elsevier.com/locate/bios

Microalgae living sensor for metal ion detection with nanocavity-enhanced photoelectrochemistry

Daniel N. Roxby [a,1], Hamim Rivy [a,1], Chaoyang Gong [a], Xuerui Gong [a], Zhiyi Yuan [a], Guo-En Chang [b], Yu-Cheng Chen [a,c,*]

[a] School of Electrical and Electronics Engineering, Nanyang Technological University, 50 Nanyang Avenue, 639798, Singapore
[b] Department of Mechanical Engineering, and Advanced Institute of Manufacturing with High-Tech Innovations, National Chung Cheng University, Chiayi, 62102, Taiwan
[c] School of Chemical and Biomedical Engineering, Nanyang Technological University, 62 Nanyang Drive, 637459, Singapore

ARTICLE INFO

Keywords:
Metal ion detection
Optical nanocavity
Photoelectrochemistry
Photosynthesis
Microalgae
Strong-coupling

ABSTRACT

Metal ions are known to play various roles in living organisms; therefore, the detection of metal ions in water resources is essential for monitoring health and environmental conditions. In contrast to artificially fabricated materials and devices, biological-friendly materials such as microalgae have been explored for detecting toxic chemicals by employing fluorescence emissions and biophotovoltaic fuel cells. However, complicated fabrication, long measurement time, and low sensitivity remain the greatest challenge due to the minimal amount of bioelectricity generated from whole-cell microalgae. Herein we report the novel concept of a microalgae living biosensor by enhancing photocurrent through nanocavities formed between copper (Cu) nanoparticles and the Cu-electrode beneath. The strong energy coupling between plasmon cavity modes and excited photosynthetic fluorescence from *Chlorella* demonstrated that photoelectrical efficiency could be significantly amplified by more than two orders of magnitude through nanocavity confinement. Simulation results reveal that substantial near-field enhancements could help confine the electric field to the electrodes. Finally, the microalgae sensor was exploited to detect various light and heavy metal ions with a breakthrough detection limit of 50 nM. This study is envisioned to provide inspirational insights on nanocavity-enhanced electrochemistry, opening new routes for biochemical detection, water monitoring, and sustainable optoelectronics.

1. Introduction

Metal ions are commonly found throughout nature and are known to play various functions in biology and living organisms (Avila et al., 2013; Cheney et al., 1995). However, the pollution of freshwater systems by heavy and light metal ions poses a significant threat to aquatic life and humans at the same time. As such, sensitive detection of metal ions from water supplies is essential for human health. Numerous methods have been developed to sense metal ions, including spectroscopy, colorimetry, and electrochemical techniques (Siddiqi et al., 2020; Chouler et al., 2019). Both optical and electrical-based techniques have seen increased interest for their high sensitivity, including the use of liquid crystals with polarised optical microscope (Siddiqi et al., 2020), whispering gallery modes (Duan et al., 2019), fluorescence probes (De Acha et al., 2019; Guo et al., 2017), and electrochemical devices (Cui et al., 2015; Reay et al., 1996; Walters et al., 2020). In contrast to artificially fabricated micro/nanomaterials, algae itself serves a model organism whose growth is sensitive to various molecules (Safi et al., 2014) and is known to produce electrical current when used with biophotovoltaic (BPV) cells (Bombelli et al., 2015; Wey et al., 2019; Saar et al., 2018; Ng et al., 2018; Roxby et al., 2020). In recent years, microbial-based sensors have been explored for the detection of toxic chemicals by employing fluorescence emissions (Durrieu et al., 2004; Wong et al., 2013; Védrine et al., 2003) and electrochemical fuel cells (Chouler et al., 2019; Wey et al., 2019; Chouteau et al., 2005; Tsopela et al., 2014, 2016). Nonetheless, most of these sensors still lack high sensitivity, rapid detection, and simplicity. Typically, device designs have incorporated biofilms and membranes, which increase design complexity, costs, and may interfere with sensitivity and measurement time.

* Corresponding author. School of Electrical and Electronics Engineering, Nanyang Technological University, 50 Nanyang Avenue, 639798, Singapore.
E-mail address: yucchen@ntu.edu.sg (Y.-C. Chen).
[1] Equal Contribution (co-first author).

https://doi.org/10.1016/j.bios.2020.112420
Received 25 April 2020; Received in revised form 13 June 2020; Accepted 30 June 2020
Available online 6 July 2020

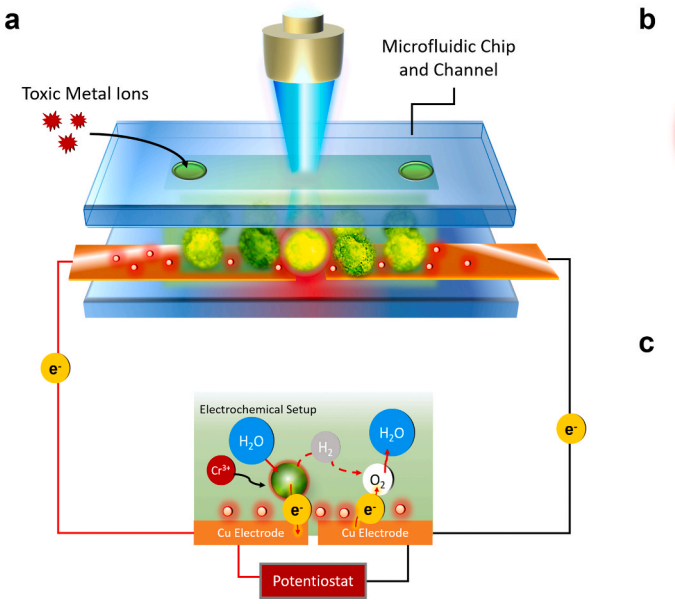

Fig. 1. Schematic illustration of the photosynthetic microalgae biosensor with nanocavity. (a) A microfluidic chip designed with a copper tape bottom layer is injected with *Chlorella sp.* and excited with violet light. Metal ions can then be injected into the device. The bottom panel shows the split copper tape electrodes to harvest electrons from *Chlorella sp.* **(b)** Concept of Fabry-Perot like nanocavity formed between nanoparticles and copper film beneath. The microalgae will absorb the reflected and scattered fluorescence emission. Strong plasmon coupling is also expected to form hotspots when the CuNPs are closely adhered to the electrode surface, therefore enhancing the photocurrents. **(c)** Photo of the sensing device in which *Chlorella sp.* are being excited by violet light. (For interpretation of the references to color in this figure legend, the reader is referred to the Web version of this article.)

When a small amount of living microalgae (*Chlorella sp.*) is embedded into an optofluidic BPV device, the photosynthetic activity of the microalgae responds immediately upon metal ions injection in water. Since microalgae only generate a small amount of electricity, it is barely possible to measure any observable photocurrent directly from whole cells. In this study, we introduce the novel concept of microalgae living biosensor for metal ion detection by boosting bio-photocurrent with copper nanocavities (Fig. 1), in which resonance is formed between Cu-nanoparticles (CuNPs) and the Cu electrode beneath. The excited photosynthetic fluorescence then generates strong energy coupling with the cavity modes, resulting in an amplification of photoelectrochemical signals. The results demonstrate that when the resonant wavelength of the nanocavities matches with the excited fluorescence of *Chlorella sp.*, the photoelectrical output would be significantly enhanced. More importantly, our findings show that nanocavity can substantially increase the photocurrent by more than two orders of magnitude. The simulation also verified resonance hot spots formed by CuNPs would help confine the electric field to the electrodes. Lastly, we exploited the algae sensor to detect various metal ions, including cadmium, iron, chromium, and manganese ions. A detection limit of 50 nM was achieved for heavy and light metal ions in water, which is three orders better than the exposure threshold defined by the World Health Organization (Environmental Prote, 1989). We envisage that this work has implications and applications for the biosensing, water recycling, bioenergy generation, and sustainable optoelectronics fields.

2. Materials and methods

2.1. Biological material preparation

Chlorella sp. (ATCCC 14854) was grown and prepared as previously described (Roxby et al., 2020). In particular, 40 μL of *Chlorella sp.* was mixed with 5 μL of CuNP solution, vortexed, and then 25 μL of this solution was aliquoted into the device. The CuNPs were purchased from Sigma Aldrich (CAS no. 7440-50-8), and solutions were prepared by adding 1 mg CuNPs to 1 ml of DI water and vortexed directly to ensure a homogenous solution. A fixed concentration of 1.18×10^8 cells/ml was used for all experiments throughout the paper. For all experiments, 25 μL *Chlorella sp.* and CuNP solution was prepared while additional 5 μL metal ion solution was added for detection.

2.2. Photoelectrochemical device and optical system measurements

To assemble the device, a thin-film copper tape (AdaFruit electronics) has adhered to a glass slide while a small cut was made to split into two electrodes. A home-made microfluidic chip with two injection holes was then adhered to the top of the glass slide and sealed with UV glue. Upon injection of the *Chlorella sp.* and CuNPs, the device was loaded into a Nikon NiE upright microscope platform for photoelectric measurements. All photoelectrochemical measurements were taken with a Zahner Zennium Potentiostat set to 0 V in chronoamperometry mode, to maximize current without biasing it. Each experiment used a fresh aliquot of *Chlorella sp.* and measured over 3 routes. Between experiments, a syringe was used to clean the channel with H_2O and air. Cadmium ($CdCl_2$), iron ($FeCl_3$), manganese ($MnCl_2$), and chromium ($CrCl_3{\cdot}6H_2O$) were purchased from Sigma Aldrich, was dissolved in DI H_2O to a concentration of 1 mg/ml, and a 1/10 serial dilution was performed down to 0.00001 mg/ml, after which 5 μL injections into the device were used.

Both for the provision of light and measurement of fluorescence, a Nikon NI-E microscope was used. A 10x objective attachment aimed at the device focused the light on the width of the chamber and had an area of 0.071 cm^2. Light from a SOLA light engine was passed through a filter cube to obtain violet light. The excitation wavelength was 375 nm–450 nm, with an average light intensity of 30 W/m^2 for all measurements in this study. An Andor Kymera 328i/Newton 970 EMCCD spectrophotometer was used to collect all fluorescence spectra.

3. Results and discussion

3.1. Nanocavity enhanced photoelectrochemistry via copper nanoparticles

The design of a living algae biosensor for metal ion detection is shown in Fig. 1a. The concept is realized through an optofluidic device containing copper electrodes (at the bottom substrate), in which *Chlorella sp.* are injected into the channel and illuminated by violet light (375–450 nm). In addition, CuNPs were prepared together to form nanocavities between the nanoparticles and the bottom electrode (Fig. 1b). Upon illumination, electricity is generated within the device. As shown in the inset of Fig. 1a, the chlorophyll-complex in microalgae harvest light energy during photosynthesis. The energy oxidizes water molecules into molecular oxygen, protons, and electrons in the photosystem and reaction centers. Most of the electrons released from

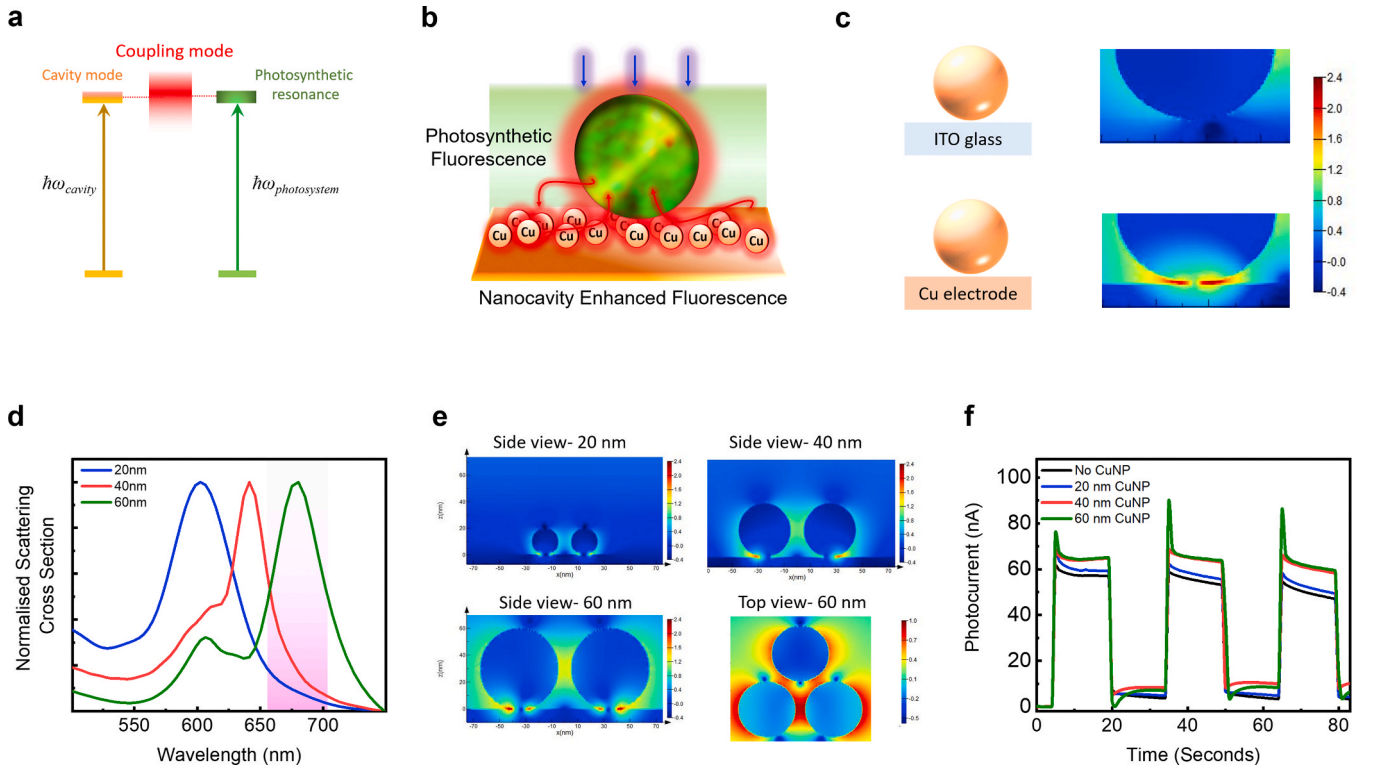

Fig. 2. Principle of nanocavity-enhanced photoelectrochemistry with Cu nanoparticles. **(a)** Energy coupling diagram between nanocavity and photosynthetic fluorescence. **(b)** Schematic showing the nanocavity-enhanced fluorescence when *Chlorella sp.* undergo violet light excitation. Fluorescence emission from the photosystem will resonance with the CuNPs and reflect back to the microalgae. **(c)** Top: Electric field distribution of 60 nm CuNPs placed above an ITO glass substrate at a wavelength of 680 nm. Bottom: Electric field distribution of 60 nm CuNPs placed on Cu electrode at a wavelength of 680 nm. **(d)** Optical simulated normalized scattering cross-section of aggregated CuNPs on Cu thin film. Normalized intensity for three copper nanoparticles of sizes 20 nm, 40 nm and 60 nm. The pink area between 660 and 710 nm shows the resonance regime. **(e)** Electric field distribution of 20/40/60 nm CuNPs at the resonant wavelength of 680 nm. The side view shows the near-field enhancement due to Fabry-Perot nanocavity formed between the CuNPs and underneath Cu tape. The top view of 60 nm shows the improvement due to the interaction of Cu nanoparticles among themself. **(f)** Photocurrent measured overtime from *Chlorella sp.* with 20 nm, 40 nm, and 60 nm copper nanoparticles in the copper nanocavity microfluidic device and illuminated with violet light. Three intervals are shown with the violet light being turned on and off for 15 s each interval. . (For interpretation of the references to color in this figure legend, the reader is referred to the Web version of this article.)

microalgae are attracted to the anode and flowed to the cathodic side through an external circuit to form electrical circuit (Thong et al., 2019). A photo of the device is given in Fig. 1c. In this work, the electrons from the microalgae cells are ferried to the electrode through direct electron transfer. When the injection of metal ions into the microfluidic channel occurs, algae interact with the metal ions, and the signal changes proportionately to the concentration of metal ions. Electrical currents are expected to increase accordingly upon interaction with metal ions. Without additional design, the magnitude of electric current generated is usually very low in free algae cells due to the cell membrane barrier.

To enhance the photocurrent generated from the algae, herein, we take advantage of nanocavities composed of CuNPs formed on Cu electrodes, as illustrated in Fig. 1b. By way of the red regime fluorescence from *Chlorella sp.*, the Cu nanocavity was designed to form optical coupling with the photosynthetic fluorescence and absorbance (Fig. S1a). The tiny nanogap between the CuNPs and the bottom copper electrode forms a nanocavity and a strong resonance in the red emission wavelengths around 680 nm due to plasmon coupling (Fig. 2a). The creation of such Fabry-Perot-like cavity was confirmed by high reflectivity at the corresponding photosynthetic resonant wavelength (Fig. S1b). Multiple reflections of emission between the CuNPs and electrode thus mimic the behavior of a Fabry-Perot resonator. This phenomenon therefore provides nanocavity-enhanced fluorescence, which can lead to enhancement of light absorption in photosystems and bioelectricity generation (Fig. 2b). This also agrees with previous work, which demonstrated that the efficiency of chemical energy production of a photosynthetic system can be strongly enhanced in the presence of plasmonic nanoparticles (Govorov and Carmeli, 2007). This fact became more explicit by comparing the electric field distribution of CuNPs adhered on low reflective substrate (ITO glass) and highly reflective substrate (Cu film). As shown in Fig. 2c (top), very weak near-field enhancement was found between CuNPs and glass substrate. This is mainly due to the low light confinement and extremely weak coupling between CuNPs and glass substrate. On the other hand, a strong near-field enhancement was observed due to the light confinement and strong plasmon coupling from the nanocavity, as shown in Fig. 2c (bottom). Different gap size and resonance enhancement were also explored in Fig. S2. Additionally, previous studies have also reported the concept of plasmonic-enhanced electrochemistry (Wang et al., 2017, 2018), indicating that electrochemical reactions can also be accelerated by plasmonic nanoparticles. As such, the nanocavity hotspots created between CuNPs and copper electrodes may assist in confining and couple electric field to the electrodes (Li et al., 2015), resulting from hot charge carriers generated during plasmon decay.

To optimize the resonance effect, optical simulations of 20 nm, 40 nm, and 60 nm CuNPs systems were evaluated in Fig. 2d. As the size of the copper nanoparticles increases, the peak intensity redshifts. Apparently, 60 nm CuNPs possess the highest spectral overlap with both the absorption and emission spectra in Fig. S1a (pink area). The near-field enhancement due to the strong CuNP-film coupling was compared under different nanoparticle sizes at 680 nm. As seen in Fig. 2e a significant near-field enhancement between the interface has been obtained at a resonant wavelength of 680 nm, where the 60 nm possess the highest magnitude. Lastly, Fig. 2f shows photocurrent generated from

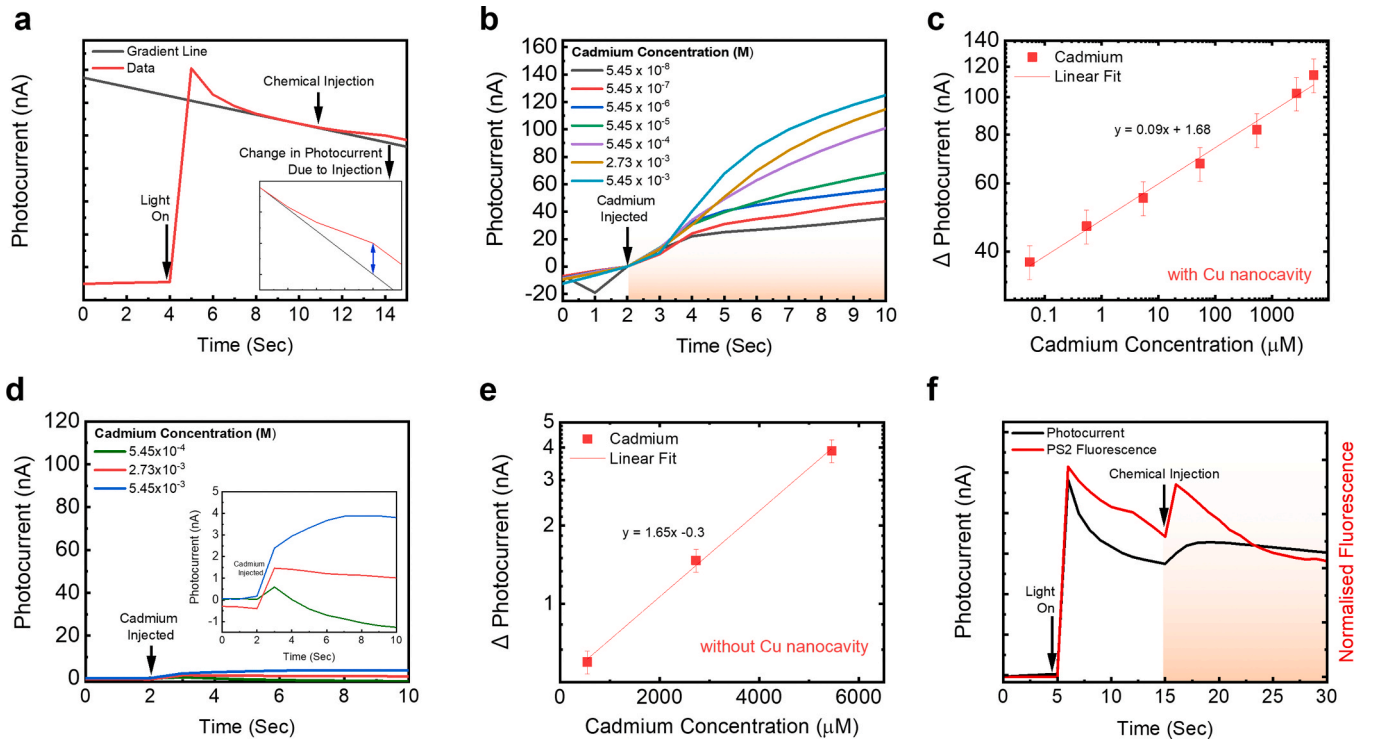

Fig. 3. Demonstration of nanocavity-enhanced metal ion sensing with photocurrents. (a) Photocurrent measured from *Chlorella sp.* (red line) in the copper nanocavity microfluidic device. At t = 4, the violet light is turned on where the photocurrent quickly rises. At t = 11, metal ions are injected, and the photocurrent increases again. The measurement is defined as the difference between photocurrent and the gradient line (black line) as shown in the inset. The gradient is defined by the nominal response in the absence of injected metal ions. Inset: a closeup illustrating the measured difference between the red and black lines. **(b)** Normalized photocurrent with nanocavity enhancement after injection of different concentrations of cadmium metal ions ($CdCl_2$). The injection occurs at t = 2, and the photocurrent rises proportionally to the concentration of the metal ions. **(c)** Summary of photocurrent increment vs. cadmium concentration (with nanocavity), both on a logarithmic scale with a standard fitting curve. The dots were based on the averages of several curves (N = 3). **(d)** Normalized photocurrent without nanocavity enhancement after injection of *extremely high concentrations* of cadmium metal ions. **(e)** Summary of photocurrent increment vs cadmium concentration (without nanocavity), both on a logarithmic scale with a standard fitting curve. (N = 3). **(f)** Photocurrent and photosystem fluorescence measured in parallel from the nanocavity microfluidic device. The metal ions are then injected at 15 s and quickly interact with the algae, resulting in further increases in the fluorescence and photocurrent. Violet LED excitation: 375 nm–450 nm. Average light intensity: 30 W/m^2. (For interpretation of the references to color in this figure legend, the reader is referred to the Web version of this article.)

Chlorella sp. in the device, by comparing with the integration of 20 nm, 40 nm, and 60 nm CuNPs. Violet light was shone on the device for 15 s, then off for 15 s, and repeated 3 times to illustrate the photoresponsive nature of the invention. In line with the scattering intensities shown in Fig. 2d, the 60 nm CuNPs peaked at 76.4 nA, the 40 nm CuNPs and 25 nm CuNPs were similar at 68.4 nA and 68.7 nA respectively, compared to 61.7 nA in the absence of any CuNPs.

3.2. *Ultrasensitive measurement of cadmium metal ions with algae sensor*

To demonstrate the capability of the microalgae biosensor, cadmium was dissolved in water to prepare a concentration of 55 nM to 5.45 mM. Fig. 3a shows a typical photocurrent signal in which the violet light is illuminated on the device at t = 4 s. Likewise, cadmium ions are injected into the microfluidic channel at t = 11 s, where an immediate increment of photocurrent was observed. The increase of photocurrent and fluorescence when metal ions interact with algae is expected (Durrieu et al., 2004; Wong et al., 2013; Védrine et al., 2003); as such, it is critical to quantify the amount of photocurrent produced. To facilitate analysis, a gradient line was plotted and is considered the nominal signal in the absence of metal ion injection. Measurement of the increase in the photocurrent is measured against this gradient line, as shown in the inset of Fig. 3a. On this basis, photocurrents were measured over 10 s upon the injection of cadmium ions with different concentrations (Fig. 3b). The injection occurs at t = 2 s while the photocurrent increases accordingly. Note that all curves in Fig. 3b are zeroed at the time of injection to aid in analysis. Summary of photocurrent increment versus cadmium concentration (with nanocavity) is further illustrated in Fig. 3c where both x- and y-axes are set to a logarithmic scale. Note that the dots in Fig. 3c was based on the averages of several curves (N = 3) for individual concentration. A linear relationship between photocurrent and cadmium concentration was observed, and a detection limit of 50 nM was identified.

In order to investigate the Cu nanocavity enhancement, photocurrent generated from *Chlorella sp.* was measured without any CuNPs deposited on the electrode. In Fig. 3d and e we can see that when 500 μM (~0.1 mg/ml) of cadmium was injected, less than 1 nA of photocurrent increment was detected. In contrast, with the addition of CuNPs (Fig. 3b), more than 100 nA of increment was achieved under the same concentration with CuNPs nanocavity. At extremely low concentrations (~55 nM), a photocurrent of 35 nA can still be measured with the enhancement of CuNPs, whilst no photocurrent was detectable at any concentrations below 100 μM without CuNPs. The findings evidently show that Cu nanocavity can significantly increase the photocurrent by more than two orders of magnitude. According to literature, toxic chemicals (or metal ions) block the electron transport between photosystems, impacting on the acceptor side of photosystem II. Consequently, a rapid increase in fluorescence occurs, in which the fluorescence intensity can be used as an indicator to verify the interaction between metal ions (Lefevre et al., 2012; Ralph et al., 2010). To validate the sensing mechanism, the photosystem fluorescence from microalgae was measured simultaneously with the photocurrent when

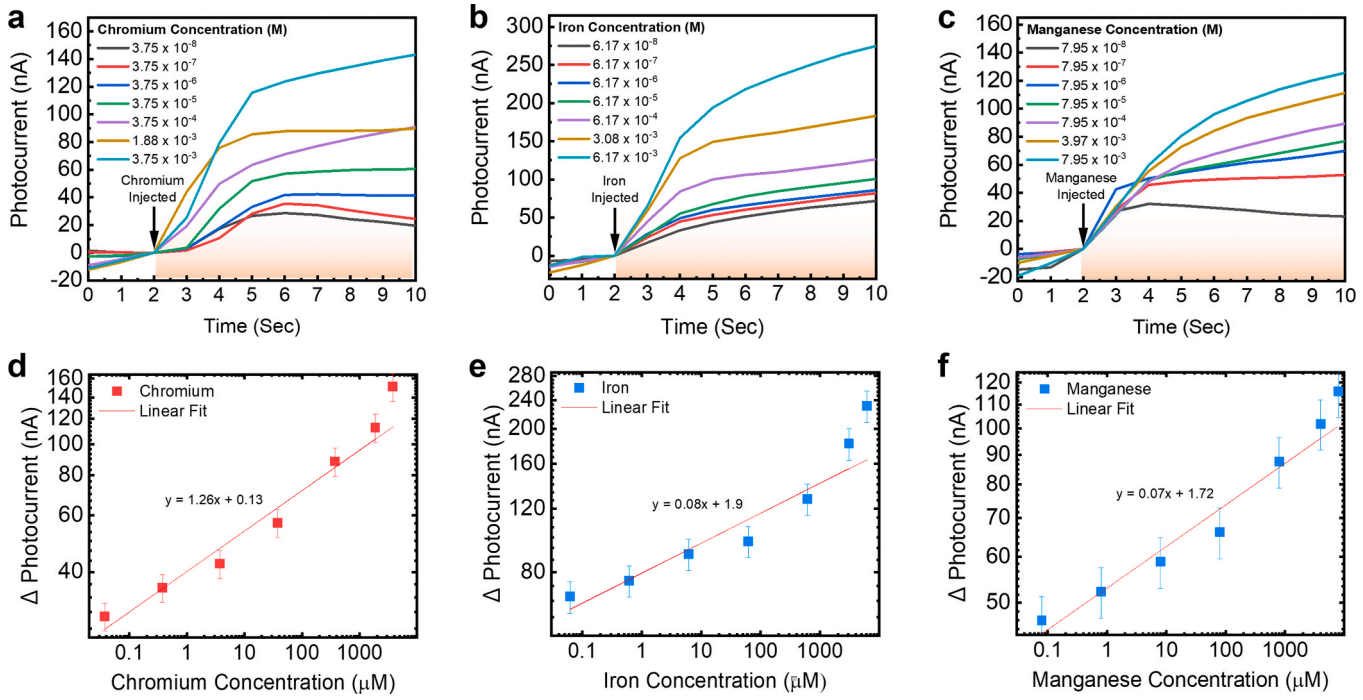

Fig. 4. Ultra-low concentration detection of heavy and light metal ions. (a) Normalized photocurrent with nanocavity enhancement after injection of different concentrations of chromium metal ions ($CrCl_3 \cdot 6H_2O$). **(b)** Normalized photocurrent with nanocavity enhancement after injection of different concentrations of iron metal ions ($FeCl_3$). **(c)** Normalized photocurrent with nanocavity enhancement after injection of different concentrations of manganese metal ions ($MnCl_2$). **(d)** Summary of photocurrent increment vs. chromium concentration on a logarithmic scale. **(e)** Summary of photocurrent increment vs. iron concentration on a logarithmic scale. **(f)** Summary of photocurrent increment vs. manganese concentration on a logarithmic scale. For all three experiments, the injection occurs at t = 2, and the photocurrent rises proportionally to the concentration of the metal ions. The dots were based on the averages of several curves (N = 3) for each concentration. The fitting standard curves and formula for (a–c) are plotted in (d–f), respectively. Violet LED excitation: 375 nm–450 nm. Average light intensity: 30 W/m^2. (For interpretation of the references to color in this figure legend, the reader is referred to the Web version of this article.)

injecting the metal ions. In Fig. 3f one can observe the photocurrent and fluorescence increasing simultaneously in response to the violet light at t = 5 s then decreases gradually. However, soon after the metal ions were injected at t = 15 s, both the fluorescence and photocurrent rapidly increase in response. This effect is consistent with other fluorescent measurements when *Chlorella sp.* are mixed with toxic molecules (Durrieu et al., 2004; Wong et al., 2013; Védrine et al., 2003) where increases in fluorescence are observed.

As an additional control group, data shown in Fig. S3a shows the effect of the injection of metal ions into the plain device (without microalgae). As seen here, the current is minimal, owing to a lack of *Chlorella sp.,* and the injection of metal ions causes the photocurrent to go in the opposite direction to that shown in Fig. 3b. In order to estimate how much variance of photocurrent will result from this disturbance, Fig. S3b shows the impact of injecting pure water into the cavity containing *Chlorella sp.* The result shows that photocurrent changes in pure water injection are minimal compared to the injection of the metal ions shown in Fig. 3b. All in all, these results elucidate that the photocurrent comes as a result of metal ions interacting with *Chlorella sp.,* which causes a change in the photosynthesis systems, the heart of *Chlorella sp.*'s electricity-generating capabilities in BPVs.

3.3. Detection of different heavy and light metal ions

To harness this capability and to extend the selection of metal ions the living algae biosensor can sense, we tested different concentrations of the iron, chromium, and manganese. All the ions were prepared under concentrations of 1×10^{-5} mg/ml to 1 mg/ml throughout all experiments. Fig. 4a shows the photocurrent for different concentrations of chromium being injected at 2 s. The chromium concentrations range from 38 nM to 3.75 mM, whilst the photocurrents range from 29.1 nA to 151.0 nA. This is further shown in Fig. 4d, which plots the photocurrent vs chromium concentration on a logarithmic scale. These same tests were then conducted with iron whereby the concentrations ranged from 62 nM to 6.2 mM with photocurrents ranging from 68.0 nA to 231.1 nA as shown in Fig. 4b and e. Lastly, the experiments were conducted with manganese as shown in Fig. 4c and f. The manganese concentrations ranged from 79 nM to 7.95 mM and the photocurrents ranged from 46.6 nA to 115.8 nA. It is clear from these results, that *Chlorella sp.* is a versatile organism that can be used for biosensing and can harness this capability to detect various metal ions.

4. Conclusions

This work has proposed the novel concept of a living algae biosensor for the detection of metal ions in water using copper nanocavities. Leveraging the energy coupling between *Chlorella sp.* and CuNPs, the electrical output of the optofluidic device was enhanced, thus increasing the sensitivity during the detection of metal ions. We first showed that by creating nanocavities through the addition of CuNPs, photocurrent could be increased by over 120%, which allows for ultra-low detection of metal ions to be improved by three-order of magnitude. After this, we showed the detection of cadmium metal ions could go as low as the nanomolar level and a linear correlation between photocurrent and cadmium concentration. The detection of chromium at each concentration occurred within a matter of seconds and is significantly faster than similar studies, which can suggest as much as 30 min for low concentration measurements. It is worth noting that without nanocavity, the photocurrent was extremely low; hence we also needed several minutes waiting to reach a measurable current. However, due to the significantly improved sensitivity with nanocavity, the required measurement time can be shortened to less than 10 s to achieve a

maximum value and a larger dynamic range. The significance of this work was further extended when it was shown that the other metal ions, namely iron, chromium, and manganese, could also be detected at the nanomolar level with this technology. In short, we would like to propose future perspectives for the optimization and realization of photosynthetic cavity-based biosensing. First, since the device is microfluidic-based, it could be used for both off- and online monitoring. Secondly, optimization could be performed for internal resistance, cavity coupling, and electrode distance to increase the sensitivity further. Thirdly, *Chlorella sp.* is sensitive to a large variety of different molecules, thus opening the possibility of testing more than just metal ions. Other biomolecules such as photosynthetic proteins or cyanobacteria that may be more sensitive or have higher selectivity between toxic chemicals.

Declaration of competing interest

The authors declare that they have no known competing financial interests or personal relationships that could have appeared to influence the work reported in this paper.

CRediT authorship contribution statement

Daniel N. Roxby: Writing - original draft, Formal analysis, Investigation. **Hamim Rivy:** Writing - original draft. **Chaoyang Gong:** Formal analysis, Investigation. **Xuerui Gong:** Formal analysis, Investigation. **Zhiyi Yuan:** Investigation, Validation. **Guo-En Chang:** Methodology. **Yu-Cheng Chen:** Supervision, Writting - original draft.

Acknowledgments

We would like to thank Professor Raymond Lau from School of Chemical and Biomedical Engineering as well as the support from University Internal Grant NAP SUG - M4082308.040. We would especially like to thank financial support from the Ministry of Education Singapore AcRF Tier 1 RG 158/19-(S).

Appendix A. Supplementary data

Supplementary data to this article can be found online at https://doi.org/10.1016/j.bios.2020.112420.

References

Avila, D.S., Puntel, R.L., Aschner, M., 2013. Interrelations between Essential Metal Ions and Human Diseases, pp. 199–227.
Bombelli, P., Müller, T., Herling, T.W., Howe, C.J., Knowles, T.P.J., 2015. A high power-density, mediator-free, microfl uidic biophotovoltaic device for cyanobacterial cells. Adv. Energy Mater. 5 (2), 1401299.
Cheney, K., Gumbiner, C., Benson, B., Tenenbein, M., 1995. Survival after a severe iron poisoning treated with intermittent infusions of deferoxamine. J. Toxicol. Clin. Toxicol. 33 (1), 61–66.
Chouler, J., Monti, M.D., Morgan, W.J., Cameron, P.J., Di Lorenzo, M., 2019. A photosynthetic toxicity biosensor for water. Electrochim. Acta 309, 392–401.
Chouteau, C., Dzyadevych, S., Durrieu, C., Chovelon, J.M., 2005. A bi-enzymatic whole cell conductometric biosensor for heavy metal ions and pesticides detection in water samples. Biosens. Bioelectron. 21, 273–281.
Cui, L., Wu, J., Ju, H., 2015. Electrochemical sensing of heavy metal ions with inorganic, organic and bio-materials. Biosens. Bioelectron. 63, 276–286.
De Acha, N., Elosúa, C., Corres, J.M., Arregui, F.J., 2019. Fluorescent sensors for the detection of heavy metal ions in aqueous media. Sensors 19 (3), 599.
Duan, R., Li, Y., Li, H., Yang, J., 2019. Detection of heavy metal ions using whispering gallery mode lasing in functionalized liquid crystal microdroplets. Biomed. Optic Express 10 (12), 6073–6083.
Durrieu, C., Chouteau, C., Barthet, L., Chovelon, J.M., Tran-Minh, C., 2004. A Bi-enzymatic whole-cell algal biosensorfor monitoring waste water pollutants. Anal. Lett. 37 (8), 1589–1599.
U. S. Environmental Protection Agency, 1989. Risk Assessment, Management and Communication of Drinking Water Contamination, Washington, DC, US. EPA625/4-89/024, EPA.
Govorov, A.O., Carmeli, I., 2007. Hybrid structures composed of photosynthetic system and metal Nanoparticles: plasmon enhancement effect. Nano Lett. 7 (3), 620–625.
Guo, J., Zhou, M., Yang, C., 2017. Fluorescent hydrogel waveguide for on-site detection of heavy metal ions. Sci. Rep. 7 (1), 7902, 2017.
Lefevre, F., Chalifour, A., Yu, L., Chodavarapu, V., Juneau, P., Izquierdo, R., 2012. Algal fluorescence sensor integrated into a microfluidic chip for water pollutant detection. Lab Chip 12 (4), 787–793, 2012.
Li, X., Ren, X., Zhang, Y., Choy, W.H., Wie, B., 2015. An all-copper plasmonic sandwich system obtained through directly depositing copper NPs on a CVD grown graphene/copper film and its application in SERS. Nanoscale 7 (26), 11291–11299.
Ng, F.-L., Phang, S.-M., Periasamy, V., Beardall, J., Yunus, K., Fisher, A.C., 2018. Algal biophotovoltaic (BPV) device for generation of bioelectricity using Synechococcus elongatus (Cyanophyta). J. Appl. Phycol. 30 (6), 2981–2988.
Ralph, P.J., Wilhelm, C., Lavaud, J., Jakob, T., Petrou, K., Kranz, S.A., 2010. Fluorescence as a tool to understand changes in photosynthetic electron flow regulation. In: Chlorophyll a Fluorescence in Aquatic Sciences: Methods and Applications. Springer, Dordrecht, pp. 75–89.
Reay, R.J., Flannery, A.F., Storment, C.W., Kounaves, S.P., Kovacs, G.T.A., 1996. Microfabricated electrochemical analysis system for heavy metal detection. Sens. Actuators, A B 34 (1–3), 450–455.
Roxby, D.N., Yuan, Z., Krishnamoorthy, S., Wu, P., Tu, W.C., Chang, G.E., Lau, R., Chen, Y.C., 2020. Enhanced biophotocurrent generation in living photosynthetic optical resonator. Adv. Sci. 7 (11), 1903707.
Saar, K.L., Bombelli, P., Lea-Smith, D.J., Call, T., Aro, E.-M., Müller, T., Howe, C.J., Knowles, T.P.J., 2018. Enhancing power density of biophotovoltaics by decoupling storage and power delivery. Nat. Energy 3 (1), 75–81.
Safi, C., Zebib, B., Merah, O., Pontalier, P.Y., Vaca-Garcia, C., 2014. Morphology, composition, production, processing and applications of Chlorella vulgaris: a review. Renew. Sustain. Energy Rev. 35, 265–278.
Siddiqi, H.M., Lin, Y. Kun, Hussain, Z., Majeed, N., 2020. Bovine serum albumin protein-based liquid crystal biosensors for optical detection of toxic heavy metals in water. Sensors 20 (1), 298.
Thong, Cheng-Han, Phang, Siew-Moi, Ng, Fong-Lee, Periasamy, Vengadesh, Ling, Tau-Chuan, Yunus, Kamran, Adrian, C., Fisher, 2019. Effect of different irradiance levels on bioelectricity generation from algal biophotovoltaic (BPV) devices. Energy Sci. Eng. 7 (5), 2086–2097.
Tsopela, A., Lale, A., Vanhove, E., Reynes, O., Seguy, I., Temple-Boyer, P., Juneau, P., Izquierdo, R., Launay, J., 2014. Integrated electrochemical biosensor based on algal metabolism for water toxicity analysis. Biosens. Bioelectron. 61, 290–297.
Tsopela, A., Laborde, A., Salvagnac, L., Ventalon, V., Bedel-Pereira, E., Seguy, I., TempleBoyer, P., Juneau, P., Izquierdo, R., Launay, J., 2016. Development of a lab-on-chip electrochemical biosensor for water quality analysis based on microalgal photosynthesis. Biosens. Bioelectron. 79, 568–573.
Védrine, C., Leclerc, J.C., Durrieu, C., Tran-Minh, C., 2003. Optical whole-cell biosensor using Chlorella vulgaris designed for monitoring herbicides. Biosens. Bioelectron. 18 (4), 457–463.
Walters, J.G., Ahmed, S., Terrero Rodríguez, I.M., O'Neil, G.D., 2020. Trace analysis of heavy metals (Cd, Pb, Hg) using native and modified 3D printed graphene/poly (lactic acid) composite electrodes. Electroanalysis 32 (4), 859–866.
Wang, C., Nie, X.G., Shi, Y., Zhou, Y., Xu, J.J., Xia, X.H., Chen, H.Y., 2017. Direct plasmon-accelerated electrochemical reaction on gold nanoparticles. ACS Nano 11, 5897–5905.
Wang, C., Zhao, X.P., Xu, Q.Y., Nie, X.G., Younis, M.R., Liu, W.Y., Xia, X.H., 2018. Importance of hot spots in gold nanostructures on direct plasmon-enhanced electrochemistry. ACS Appl. Nano Mater. 1 (10), 5805–5811.
Wey, L.T., Bombelli, P., Chen, X., Lawrence, J.M., Rabideau, C.M., Rowden, S.J.L., Zhang, J.Z., Howe, C.J., 2019. The development of biophotovoltaic systems for power generation and biological analysis. ChemElectroChem 6 (21), 5375–5386.
Wong, L.S., Lee, Y.H., Surif, S., 2013. Performance of a cyanobacteria whole cell-based fluorescence biosensor for heavy metal and pesticide detection. Sensors 13 (5), 6394–6404.